

Final Technical Report – Submitted Monday, November 8, 2021

USGS Cooperative Agreement Number: G19AC00287

Title of award:

Incorporating Real-Time GNSS into ShakeAlert: Improving Telemetry and Upgrading to Multi-Constellation GNSS with Onboard Positioning at Existing NOTA Stations

Author(s) and Affiliation(s) with Address and zip code. Author's telephone numbers, fax numbers and E-mail address:

Glen S. Mattioli, mattioli@unavco.org, 303-381-7554, Principal Investigator

Karl Feaux, feaux@unavco.org, 303-381-7554

Doerte Mann, mann@unavco.org, 707-364-8618

Tim Dittmann, dittmann@unvco.org, 303-381-7643

James Downing, downing@unavco.org, 303-381-7559

UNAVCO, Inc.

6350 Nautilus Drive, Boulder, CO 80301

Fax 303-381-7501

Kathleen Hodgkinson (departed UNAVCO June 4, 2021), kmhodgk@sandia.gov, 575-520-0912

Sandia National Laboratories

1515 Eubank Blvd SE, Albuquerque, NM 87123

Term covered by the report

August 15, 2019 – August 14, 2021

Abstract

This final report summarizes the work completed by UNAVCO as part of the U.S. Geological Survey (USGS) Cooperative Agreement G19AC00287. UNAVCO has enhanced its geodetic equipment and real-time data infrastructure to support the integration of real-time GNSS data from existing Network of the Americas (NOTA) stations into the USGS ShakeAlert Earthquake Early Warning (EEW) system for high-risk regions in Washington, Oregon, and Northern California.

77 NOTA stations were visited for a variety of upgrades and modernizations: 65 GPS-only receivers (Trimble NetRS) were replaced with Septentrio PolaRx5 receivers with full multi-constellation GNSS capability, and 57 GPS antennas were replaced with full-spectrum GNSS antennas. At 29 stations, older technology cell modems were replaced with modern systems using the latest 4G LTE technology. In addition, 5 new GNSS stations were built in Oregon to densify coverage in an area previously identified to need better coverage to serve the ShakeAlert system.

Onboard Precise Point Positioning (PPP) licenses were installed at 184 NOTA GNSS receivers, 150 SECORX licenses on Septentrio PolaRx5 receivers, and 34 Trimble RTX licenses at sites with existing Trimble NetR9 receivers. Receivers were configured for logging as well as transmitting these corrected positions in real-time.

As a result of these upgrades, all NOTA GNSS stations in California, Oregon, and Washington, that are located between the San Francisco Bay Area and the Canadian border, and west of Interstate 5, are now equipped with full spectrum GNSS receivers and antennas, modern telemetry, and onboard Precise Point Positioning.

Metrics from all real-time streams have been analyzed, including receiver BINEX, receiver onboard PPP estimates, and PPP estimates generated from the BINEX streams at the Boulder data center. Real-time completeness and latencies fall within expected ranges, with only the data center generated positions for NetR9 receivers showing any significant delay, with 99% completeness at 505 ms versus 272 ms for the PolaRx5 receivers.

The comparison between onboard versus data-center-generated positions has yielded some interesting observations: while noise levels of the NetR9 onboard PPP estimates are comparable to those from the data center, noise levels of the PolaRx5 PPP estimates differ significantly - these show significantly more drift (or variance) at periods of ~800 seconds but have much lower variance than any other solution type at all periods less than that. The mechanisms behind this are still under investigation, and the response of the PolaRx5 receiver and its PPP position estimate that arise from significant displacements expected for M6 or greater earthquakes should be evaluated further before onboard solutions are ingested by a production EEW system.

Overview

Great earthquakes and ensuing tsunamis in Sumatra, Chile, and Japan have demonstrated the need for accurate full spectrum ground displacements that characterize the large amplitudes and broad dynamic range associated with these complex ruptures. Large static offsets available from GNSS displacement time series provide the best early indication of the large moment release in the events; the characteristics of the source rupture that influence intermediate period ground motions between the static and about 5-10 s remain poorly known because of the poor performance of accelerometers in this range. Merging data from GNSS and seismic sensors minimize intrinsic weaknesses in both observations and provide the optimal results for earthquake source imaging and EEW. The July 2019 Ridgecrest earthquake sequence in California, and consecutive earthquake events have shown the immense value of geodetic data in determining earthquake magnitude and rupture characteristics in real-time.

Key elements for successful integration of GNSS data into ShakeAlert are the robust and reliable data transmission before, during, and immediately after a large seismic event, and the tools to process the data in real time. Also, quality assessment of a new data type, the onboard PPP solutions, is crucial for using this data in the operational EEW system. Accordingly, the following tasks were completed under this Cooperative Agreement.

1. NOTA station infrastructure upgrades

We identified NOTA stations in the Pacific Northwest target area that needed upgrades to their GNSS capabilities, cell modem telemetry, and power systems. The goal was to upgrade all sites to full spectrum GNSS receivers and antennas, and modern 4G LTE cell technology. 65 GPS-only Trimble NetRS receivers were replaced with full-GNSS Septentrio PolaRx5 receivers, and 62 sites received new full-spectrum GNSS antennas. In addition, cell modems were upgraded to new technology at 29 of these stations, and new batteries were installed to maintain adequate station power when necessary. In total, 82 NOTA sites were visited to complete these upgrades (Fig 1). Further infrastructure upgrades, the enabling of onboard Precise Point Positioning, are discussed in Section 3 below.

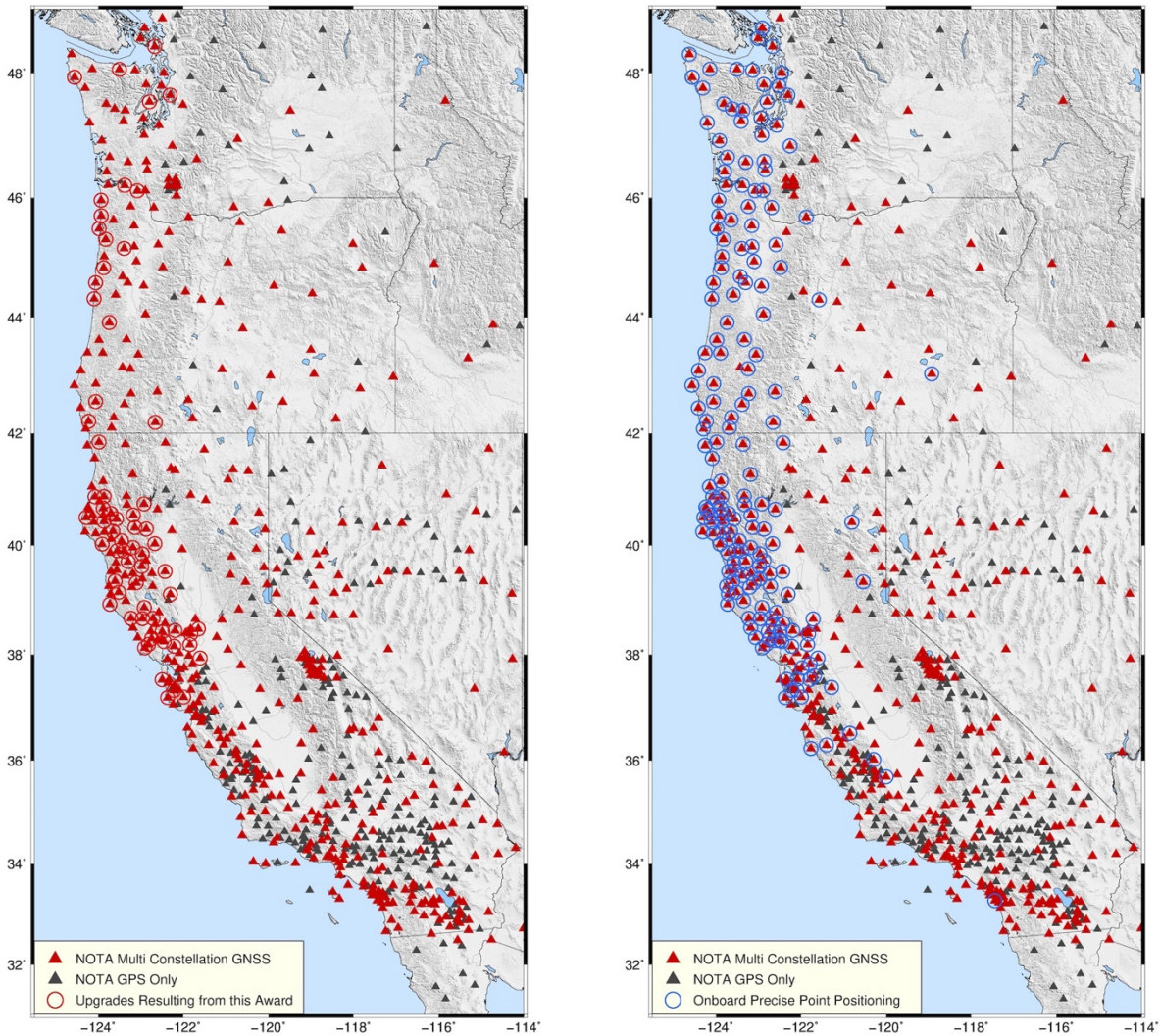


Figure 1. Left: GNSS capabilities of NOTA stations in the Pacific Northwest as of August 14, 2021, the end of the Cooperative Agreement. Red circles indicate stations that were upgraded with funds from this award. Right: GNSS capabilities of NOTA stations in the Pacific Northwest (same as on left). Blue circles indicate stations that had onboard Precise Point Positioning enabled (see Section 3 below).

2. 5 new GNSS station installations in Oregon

To densify the GNSS network in central coastal Oregon, where a significant spatial gap had been identified, 5 new GNSS stations were sited, permitted, and built (Figure 2). Two of the new stations (EUCH, NOSE) are directly collocated with seismic instrumentation (UO.UCHR and UW.RNO2 respectively) operated by the Pacific Northwest Seismic Network (PNSN). Another station, YACH, is within 3 km of seismic station UW.YACH. Different siting requirements did not allow for a direct collocation of GNSS equipment with the seismic station in this case. For an overview of station characteristics, see Table 1.

All stations are built with high precision geodetic monuments. One monument (NOSE) is a short drilled braced monument (SDBM), and the other four are shallow braced, non-drilled monuments (SBM). All new OR stations have Septentrio PolaRx5 receivers, and multi-spectrum Tallysman Verachoke antennas (VC 6050) installed. All stations use cell modems for data telemetry and operate on DC solar power with batteries. At NOSE, the power system as well as equipment enclosure is shared with PNSN.

Data for these five new sites, although not part of the NSF-funded NOTA network, are archived at UNAVCO (<https://www.unavco.org/data/gps-gnss/gps-gnss.html>). Real-time streams from these stations can be accessed through the UNAVCO NTrip caster rtgpsout.unavco.org in BINEX, RTCM3 or PPP format (see <https://www.unavco.org/data/gps-gnss/real-time/real-time.html> for more details on real-time data access)

Site ID	Site Name	Lat	Lon	Monument	Install Date	Seismic Collocation
AGNS	AgnessRR_OR2021	42.5527	-124.0591	SDBM	6/17/2021	None
EUCH	EuchreMtn_OR2021	44.8347	-123.8708	SDBM	3/30/2021	UO.UCHR
MZNT	Manzanita_OR2021	45.7015	-123.9309	SBM	7/28/2021	None
NOSE	RomanNose_OR2021	43.9121	-123.7390	SDBM	4/01/2021	UW.RNO2
YACH	YachatsCR_OR2021	44.2929	-124.0804	SBM	5/11/2021	UW.YACH

Table 1. List of 5 new GNSS sites in Oregon. SDBM: Short Drilled Braced Monument. SBM: Shallow Braced Non-Drilled Monument. Collocations refer to seismic stations operated by the Pacific Northwest Seismic Network. Note that YACH and UW.YACH are approximately 2.7 km distant from each other due to difference in siting criteria.

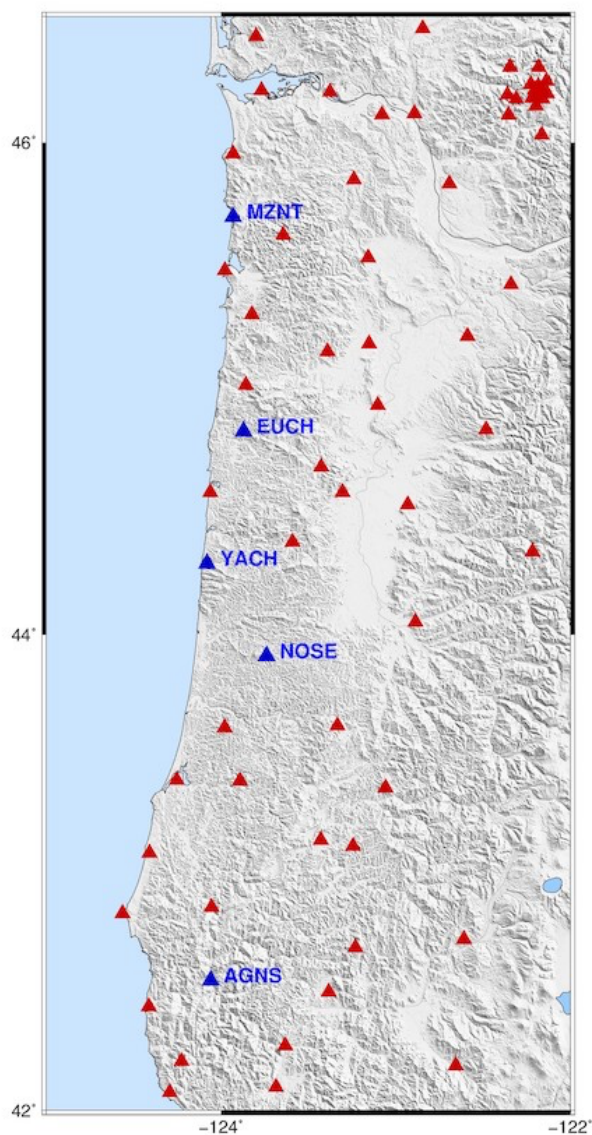


Figure 2: Map shows the locations of five newly installed GNSS stations (blue triangles), MZNT, EUCH, YACH, NOSE, AGNS, in relation to existing NOTA stations in Oregon (red triangles). Overview photos show YACH (bottom left), MZNT, EUCH, NOSE, AGNS (top to bottom on right)

3. Onboard Positioning

After completion of the GNSS upgrades, onboard positioning licenses were purchased from Trimble and Septentrio for all receivers in the target area, and the receivers were configured for using this service - onboard orbit/clock corrections are received through the GNSS antenna's L-band, and then generate corrected position estimates in real-time on the receiver.

	Septentrio PolaRx5	Trimble NetR9	Trimble Pivot Server
Num. Onboard PPP Subscriptions	150	34	184
Correction Service	Septentrio SECOR-X	Trimble RTX	Trimble RTX- server
Corrections Transmission	L-Band	L-Band	Network
Constellations Used	GPS + GLO	GPS + GLO + GAL	GPS + GLO
Receiver Tracking/PPP Filter Configuration	Level: <i>Moderate</i> Motion: <i>EarthquakeMon</i>	Signal Tracking Bandwidth: <i>Wide</i> Receiver Motion: <i>Kinematic</i>	Mode: <i>Kinematic</i> (no filtering)
1 sps PPP Stream Format	NMEA-0183 GGK and GST <ul style="list-style-type: none"> Position Time Position Lat, Lon, Ht Quality Indicator Number of SV in Fix DOP RMS of Pseudorange Residuals Error ellipse (semi major, semi minor, orientation) 1 sigma error (lat,lon,ht) 	Trimble GSOF <ul style="list-style-type: none"> Delta ECEF Lat,Lon,Ht Position Sigma Position Time Position VCV Position Type Info TPlane ENU ECEF Position LBand Status Info 	NMEA-0183 GGKxx <ul style="list-style-type: none"> Position Time Position Lat, Lon, Ht Quality Indicator Number of SV in Fix DOP Sigma (lat,lon,ht)
Local Receiver Buffer	7 days of 1 sps NMEA streams (GGK and GST)	5 sps positions embedded in native high-rate observation files (.T02) ~7 days buffer	-na-
Storing native PPP Streams?	Yes	Yes	Yes

Table 2. Receiver onboard and server generated PPP characteristics and configurations.

Position data from these receivers are being streamed at a rate of 1 sample per second in GSOF format (Trimble NetR9 receivers) or NMEA format (Septentrio RX5 receivers) to the UNAVCO data center. The 184 stations that have been equipped with onboard positioning are shown in Fig 1 (right) above. A summary of the characteristics and receiver configurations settings is shown in Table 2.

There were several challenges related to implementing this service, both for Trimble and Septentrio receivers. For example, Trimble receivers located at some coastal locations seem to require a different service that can access corrections from a satellite usually used for positioning on the marine sector. However, this service was never made available to us, resulting in a couple stations with Trimble NetR9 receivers (CHZZ, PTSG) that are currently not creating on-board positions.

Some Septentrio receivers experienced a bug reverting the positioning mode from Precise Point Positioning (PPP) to the much less accurate SBAS mode. This issue was identified using the QC metrics in Section 5 of this report, brought to Septentrio's attention, and addressed in a new firmware version (5.4.0).

4. Comparison of Onboard and Data Center Real-Time GNSS Solutions

Completeness and Latency

A test site was built at the NOTA GNSS station in Aliso Creek, California to enable comparisons of metrics among the Trimble NetR9 and Septentrio PolaRx5 receivers, each with their distinct correction services, and the UNAVCO data center solutions. A Trimble NetR9 and PolaRx5 were connected to one antenna via a splitter (Figure 3). This shared radio frequency (RF) front-end means that nominally the same RF signal was fed into the two receiver models to independently track simultaneously. GNSS multi-frequency pseudorange and phase measurements are processed at 1 sps by each receiver and the PPP estimates are streamed to Boulder. 1 sps phase and pseudorange observables were encoded into BINEX and these also were streamed to Boulder for data center processing.

To compare the latency and completeness of the solutions, we tracked the difference between the observation epoch time with the arrival times of the BINEX streams in Boulder, the arrival of the onboard PPP estimates in Boulder, and the availability of the data center solutions. In Figure 4, the dashed lines show the latency measurements for the PolaRx5 receiver, while the solid lines show the latency for the NetR9 receiver. The latencies are low for all stream types; in addition, all streams are 99.9% complete at 600 ms *i.e.*, 99.9% of all expected solutions are available within 600 ms of raw measurements being recorded on the receiver. The latencies of the PolaRx5 are lower than that of the NetR9 for all three stream types. The BINEX stream from the PolaRx5 (dashed black line) is 99% complete at 132 ms, while the NetR9 BINEX (solid black line) is 99% complete at 225 ms. The data center solutions from the NetR9 also have higher latencies being 99% complete at 505 ms compared to 272 ms for the PolaRx5. The latencies of the onboard solutions are essentially the same for both receivers (green lines) and thus are difficult to distinguish in Figure 4. We note that the onboard NetR9 solutions seem to arrive faster than the

BINEX stream from that receiver. While this result seems counter-intuitive to us, it is likely related to the order in which data is queued for streaming in the receiver firmware. These relatively rapid NetR9 PPP arrival times also indicate that there is not a significant receiver latency bias from a possible network telemetry correlation. There seems to be no loss in completeness and no increase in latency in the onboard PPP solutions when compared to the data center solutions for either of the receivers. Another interesting feature that is evident in Figure 4 is the significant lag in the NetR9 data center PPP estimates. The cause of this delay is still under investigation.

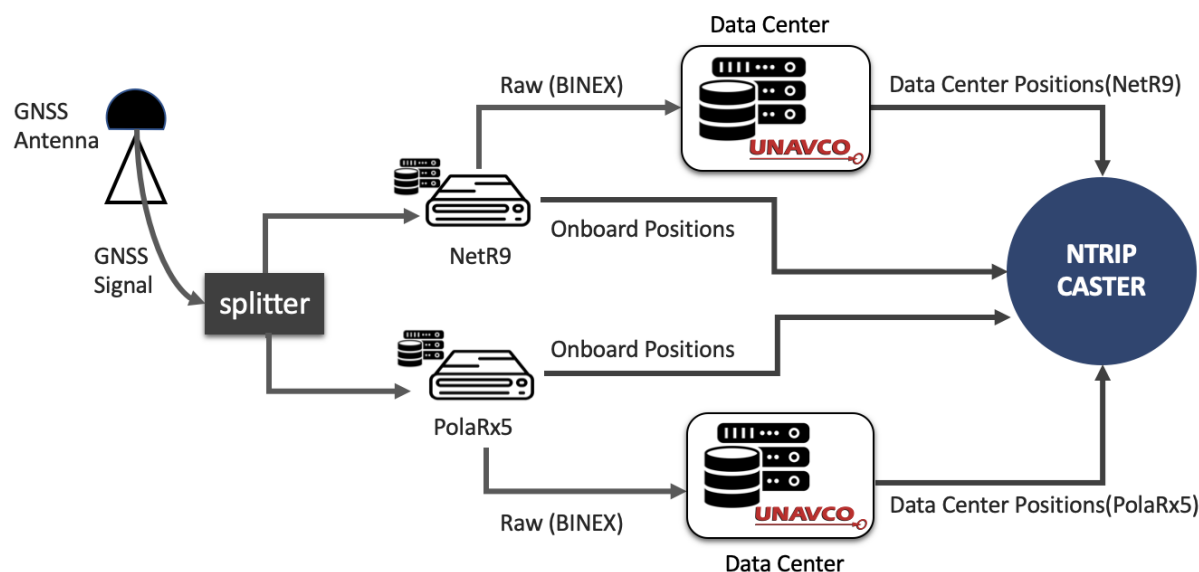


Figure 3. Schematic of test station at Aliso Creek, California. Trimble’s CENTERPOINT RTX and Septentrio’s SECORX corrections are obtained directly through the GNSS antenna. Once available, the PPP solutions would be redistributed to end-users via an NTRIP caster hosted by the UNAVCO NOC.

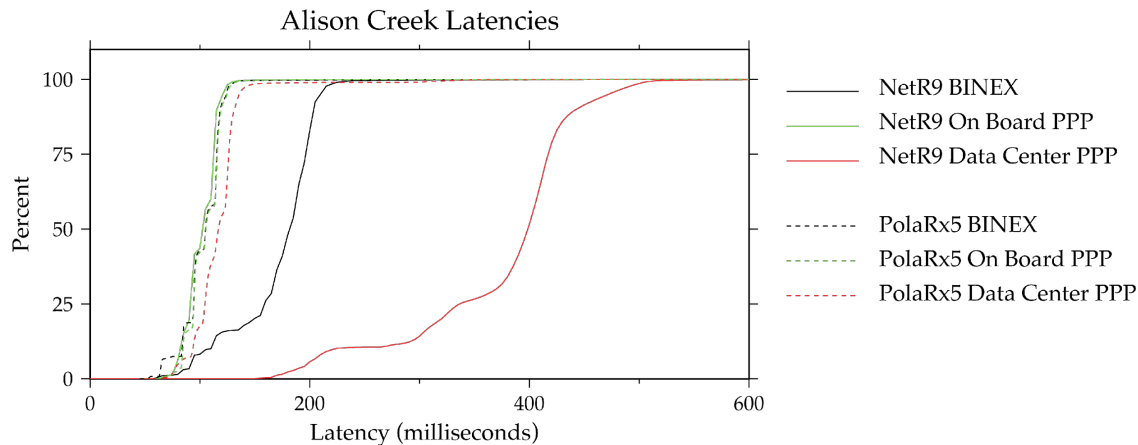
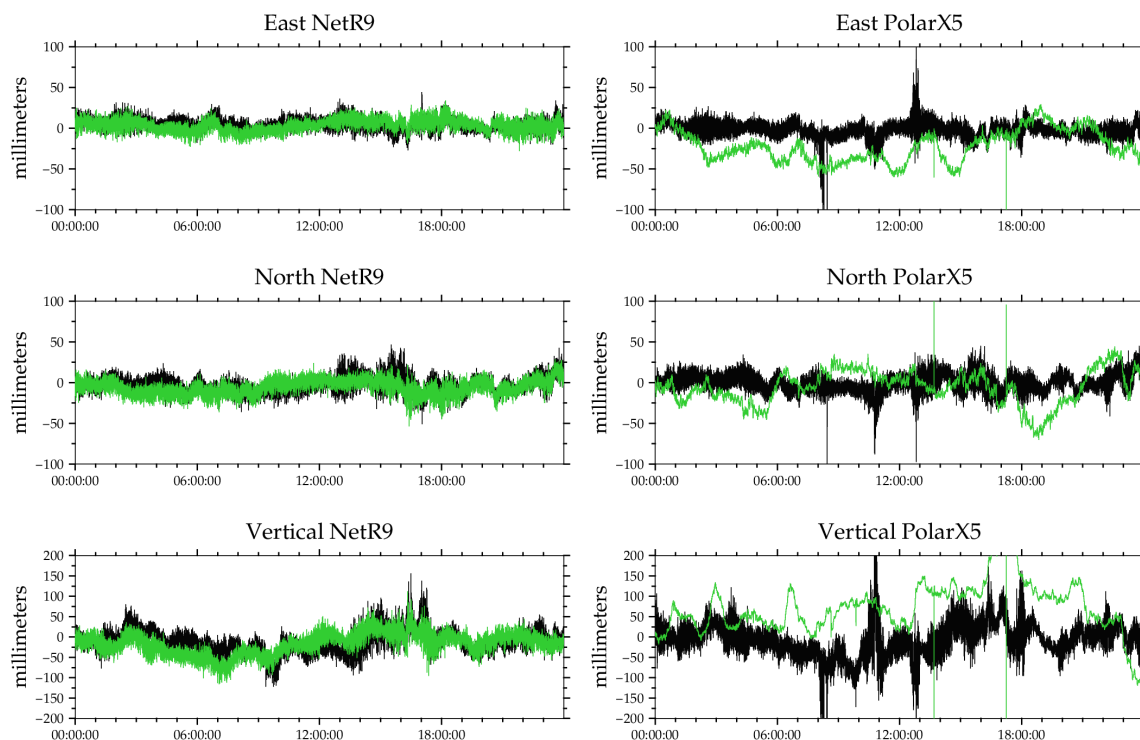


Figure 4. Latencies of streams from the Aliso Creek dual-receiver test site. Solid lines show latencies of the Trimble NetR9, while dashed lines show those of the Septentrio PolarX5. The data were collected over 24 hours on April 1, 2021.

Data Quality

In this section, we quantify the difference between the PPP estimates based on solution type. Figures 5A and 5B show the PPP estimates recorded at the Aliso Creek dual-receiver test site. The incoming BINEX streams from both receiver types are transmitted to the UNAVCO data center and ingested into the Boulder NOC processing system, Trimble PIVOT RTX, simultaneously. Black traces show the data center solutions for the NetR9 and PolaRx5, while the green traces represent the onboard solutions. The NetR9 receivers have essentially the same software as is used at the data center. In addition, both the NetR9s and the UNAVCO data center are receiving the same Trimble CENTERPOINT RTX corrections. These results provide a good indication of the expected differences in PPP estimates if the data center processing was pushed to the network edge.

By examining Figure 5, it is clear that the onboard and data center PPP estimates for the NetR9s are qualitatively similar in terms of noise characteristics, while the PolaRx5 PPP estimates differ significantly from those of the data center. In the Aliso Creek dual-receiver experiment shown in Figure 5, however, we are not only comparing different receivers, but also different processing software and real-time clock and orbit corrections. Their most notable difference is the increase in long period drift in the PolaRx5 onboard solutions (Figure 5A) combined with less scatter over



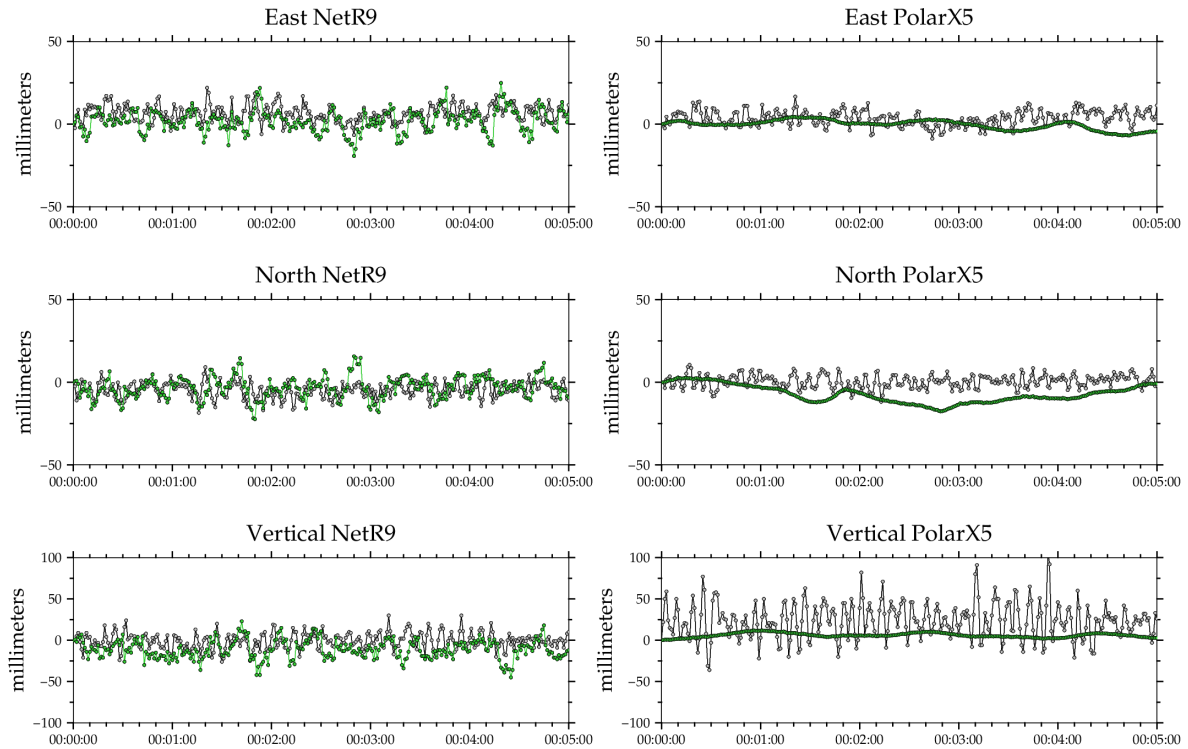


Figure 5. The east, north, and vertical displacements from the test site at Aliso Creek through April 1, 2021, A (upper six panels) 24 hours of data; B (lower six panels) 5 minutes of data. Black traces represent data center solutions, while green traces show the onboard PPP estimates for each receiver.

short periods (Figure 5B). When the PolaRx5 BINEX is processed at the data center using the RTX software both effects are greatly reduced but it is not possible to distinguish whether the different noise characteristics are caused by the onboard software or the SECORX corrections. Although the data center processing nominally uses the same BINEX observations, these results also differ. For example, in Figure 5A there are significant outliers in the data center PolaRx5 solutions that are not observed in any of the NetR9 streams.

To examine whether the Aliso Creek dual-receiver experiment was representative for the entire set of RT-GNSS NOTA stations, we computed the Median Absolute Deviation (MAD) scatter of all receivers with onboard PPP enabled on April 1, 2021 (Figure 6). For the NetR9s there is little difference in the MAD for data center and onboard over the 24-hour window (upper plots in Fig. 6). In contrast, there are significant differences for the PolaRx5 (lower plots in Fig. 6). This indicates the long-period wander observed at Aliso Creek is also observed across the network. The MAD of the data center solutions is typically about 10 mm for the horizontal components and twice that in the vertical component of the position estimate for the data center and the NetR9 PPP estimates. For the PolaRx5 receivers, the data center MAD estimates are similar to those of the NetR9 receivers, but the onboard PPP estimates show significantly higher MAD on the order of 20 mm in the horizontal components and 50 mm in the vertical component.

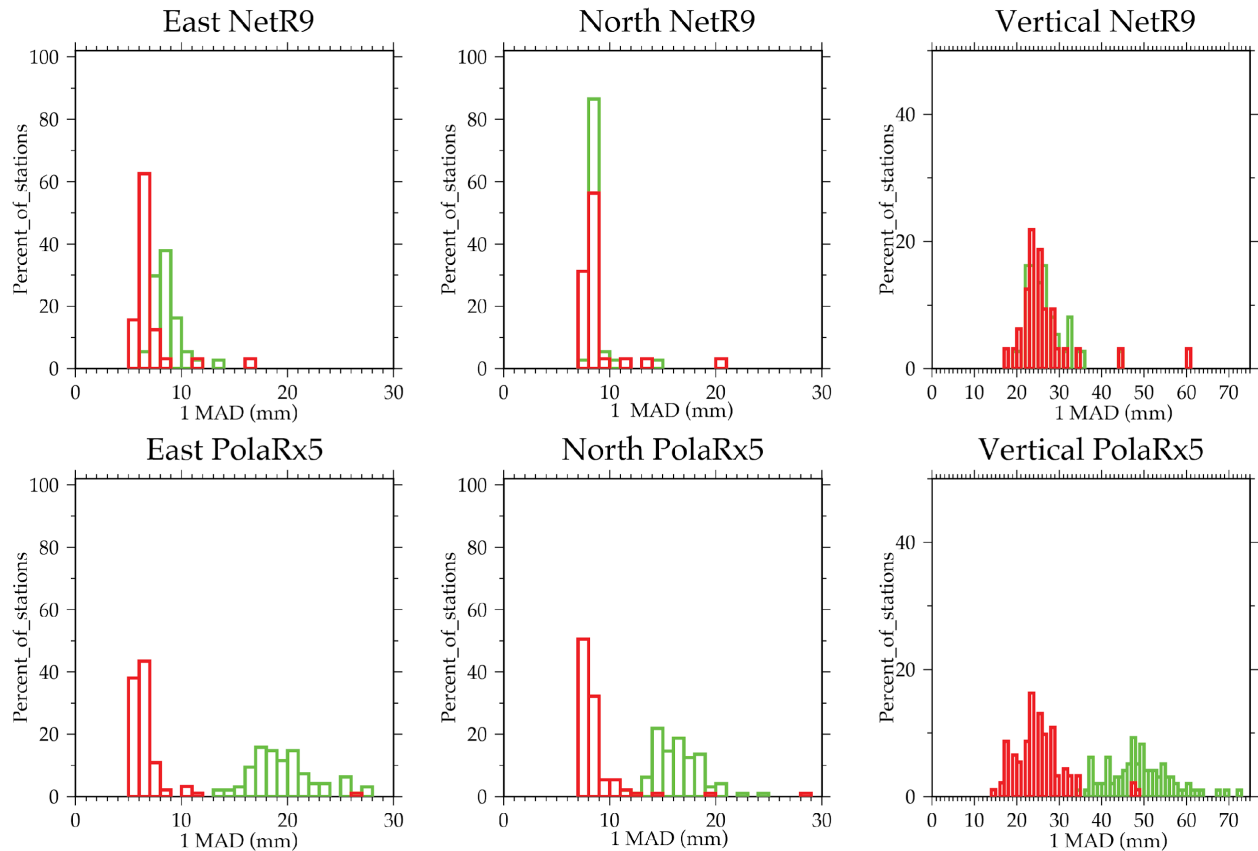


Figure 6. 24-hour 1-Median Absolute Deviation (MAD) scatter of timeseries for data center (red) and onboard (green) PPP estimates. Upper plots show the results for the NetR9 receivers ($n=39$), while the lower plots the results for the PolARx5 receivers ($n=93$). Data collected on April 1, 2021 (see Figure 5A).

It is useful to examine the apparent drift in the solutions by examining the root-mean-scatter over a range of time windows (*i.e.*, periods) across the various PPP estimates. The drift is meaningful for EEW as it quantifies the scatter of the PPP estimates across a range of observation periods. Any dynamic displacements caused by an event (*e.g.*, an earthquake) must exceed this drift for a peak ground displacement to be distinguishable from the ambient noise at any RT-GNSS station. The variance or drift in the position estimates shown on the time-series plots is quantified further in the drift plots (Figure 7). The PolARx5 onboard solutions show significantly more drift at periods of ~ 800 seconds but have much lower drift levels than any other solution type at all periods less than that. The PolARx5 data center solutions (black dashed lines) show significantly increased noise levels compared to the NetR9 data center solutions in the east and vertical components. The NetR9 onboard (solid green) and data center solutions (solid black lines) have similar levels of drift in the horizontal components. Similar results are found when the positions are analyzed in the frequency domain, where it is clear that short period signals have been suppressed in the PolARx5 solutions (Figure 8).

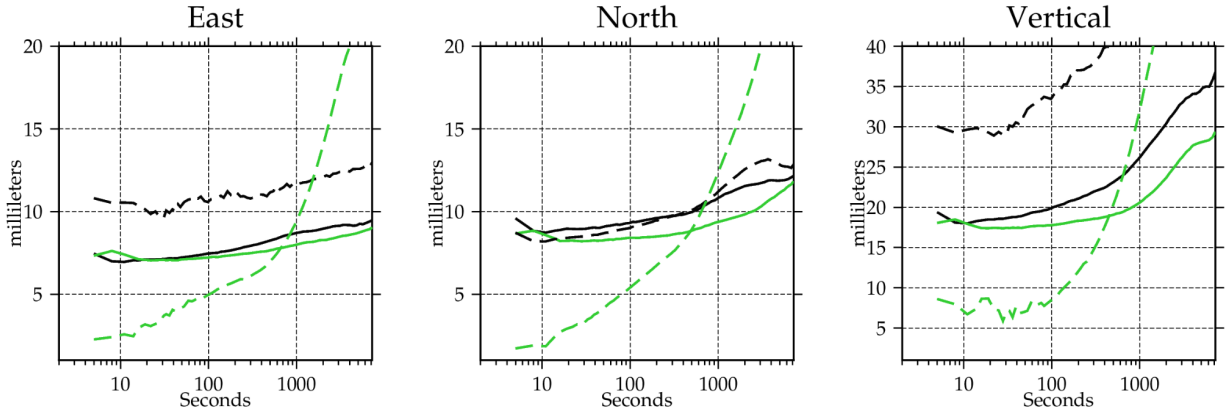


Figure 7. Drift plots for the NetR9 and PolaRx5 at Aliso Creek (Figure 5A). Solid lines show the NetR9 PPP estimates, while the dashed lines show the PolaRx5 PPP estimates. Black lines are data center solutions, while green lines are the onboard solutions.

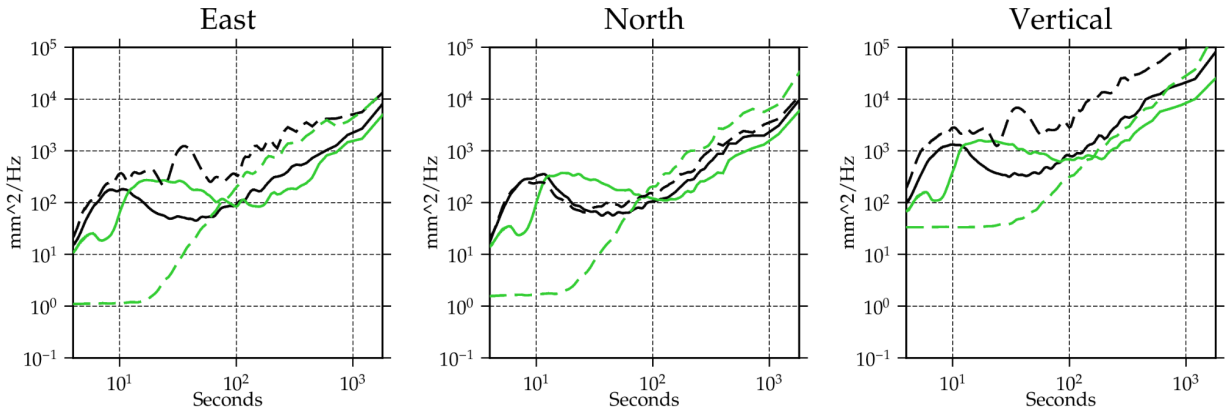


Figure 8. Power spectral density plots of positions shown in Figure 5A, calculated using 1-hour segments with 50% overlap of each segment. Lines and colors are the same as in Figure 7.

Next, we examine the drift metrics across the network by calculating the drift in mm at periods of 300 seconds (Figure 9). At that period there is minimal difference between the NetR9 and data center solutions (upper plots Fig. 9). The PolaRx5 onboard PPP estimates show significantly lower drift levels (lower plots in Fig. 9) than observed for either the NetR9 data center or onboard PPP estimates; however, this does not necessarily suggest the PolaRx5 solutions are better. In fact the question arises about how these PPP estimates are being smoothed or filtered and what impact this may have on the PolaRx5 receiver's ability to track the dynamic signal that would arise during a large magnitude earthquake.

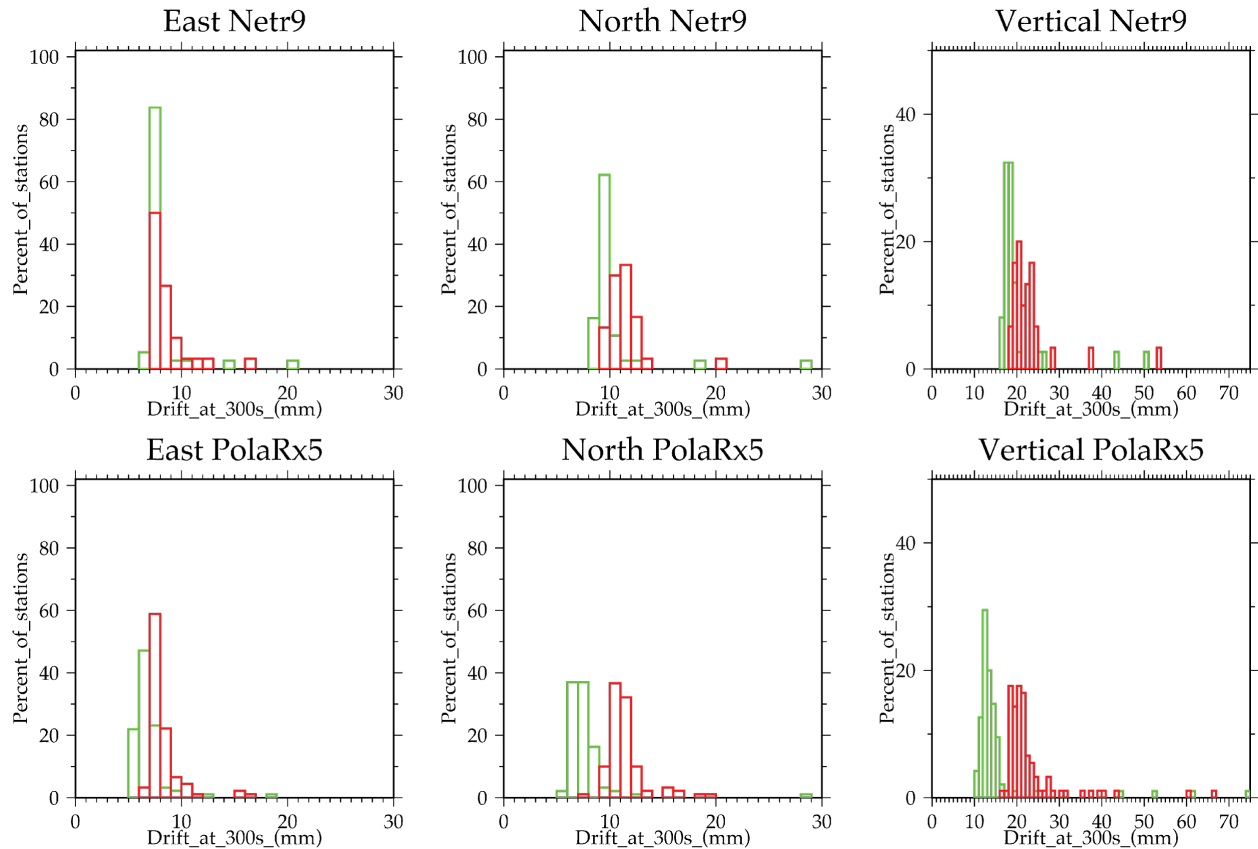


Figure 9. Drift at 300 seconds for data center (red) and onboard (green) PPP estimates. Upper plots show the results for the NetR9 receivers (n=39), while the lower plots the results for the PolaRx5 receivers (n=93). Data collected on April 1, 2021 (see Figure 5A).

Unlike UNAVCO’s real-time data center system, none of the onboard receivers have been subject to the dynamic displacements generated by an earthquake. Accordingly, we can state now that noise levels of the NetR9 PPP estimates are comparable to those of the data center, although outstanding questions remain regarding the onboard PolaRx5 PPP estimates. The response of the PolaRx5 receiver and its PPP position estimate that arise from significant displacements expected for M6 or greater earthquakes should be determined before onboard solutions are ingested by a production EEW system. In the absence of a geophysical event such as the 2019 Ridgecrest earthquake sequence, we recommend that the PolaRx5 receivers undergo rigorous shake table testing.

5. Real-Time data flow QC, QC tool development, and data availability

Real-time data flow QC and Tool Development

UNAVCO monitors completeness and latency of the raw RT-GNSS data streams plus the scatter and drift in the outgoing Precise Point Position (PPP) solutions. These have been collated on ShakeAlert web pages at UNAVCO (Table 3). The tables with information on completeness and latency are updated hourly. The scatter plots are updated at 10 second intervals and the drift plots daily. The onboard receiver PPP comparisons with the server-based PPP are updated daily. Much

of the information is presented for 30-day intervals on the web pages. The measurements are saved for long-term engineering analysis in UNAVCO's real-time database.

Quantity	Presentation	Update Generation	Link
Latency	Map view	Hourly	http://gaia.unavco.org/streamStatus/RT-GPS/mapsLatency_SA.html
	Cumulative percentile versus time	Hourly	http://gaia.unavco.org/streamStatus/RT-GPS/plotLatency_SA.html
	Time-series	Hourly	http://gaia.unavco.org/streamStatus/RT-GPS/plotLatency_SA.html
	Tabular form	Hourly	http://gaia.unavco.org/streamStatus/RT-GPS/RegionSummary.ShakeAlert.html
Completeness	Cumulative percentile versus time	Hourly	http://gaia.unavco.org/streamStatus/RT-GPS/RegionSummary.ShakeAlert.html
PPP Solutions	Scatter plots	10 s	http://gaia.unavco.org/streamStatus/RT-GPS/plotGPSScatter6_SA.html
	Time-series plots	10 s	http://gaia.unavco.org/streamStatus/RT-GPS/plotGPS.html
	Drift plots	Daily	http://gaia.unavco.org/streamStatus/RT-GPS/Wander.html
Onboard PPP versus Server PPP Comparisons	Time-series plots	Daily	http://gaia.unavco.org/streamStatus/RT-GPS/onBoard_timeSeries.html
	Scatter-plots	Daily	http://gaia.unavco.org/streamStatus/RT-GPS/onBoard_scatter.html
	PSD plots	Daily	http://gaia.unavco.org/streamStatus/RT-GPS/onBoard_psd.html
	Combination plots	Daily	http://gaia.unavco.org/streamStatus/RT-GPS/onBoard.html

Table 3. Summary of ShakeAlert Station Monitoring at UNAVCO

a) Latencies and Completeness

The incoming latencies are measured as each observation arrives at UNAVCO's NOC in Boulder. These epoch-by-epoch values are then averaged hourly and presented in a map view with an option to change the date and time (see Table 3 for links). This allows network operators to view latencies in a spatio-temporal manner. The latencies are also presented for each station in terms of cumulative percentage completeness and as a temporal chart where they can be viewed in the context of the overall NOTA network performance (e.g., Figure 4). Presenting the information for

all sites allows identification of common problems across the network. The latencies are also presented in a color-coded tabular form where problematic sites can be quickly identified.

Completeness is summarized in two ways: 1) as a count of the number of epochs that arrive at the UNAVCO NOC regardless of the length of time it takes to arrive; and 2) as a function of latency (Figure 4, Table 3). This latter metric allows analysis of the state of health of the communications pathways between the receiver and the NOC. While the first metric allows operators to know how much data has streamed from the station, the second provides a measurement of how much data arrived within a certain time interval. The total count is summarized in tabular form as a color-coded table and in a temporal map view.

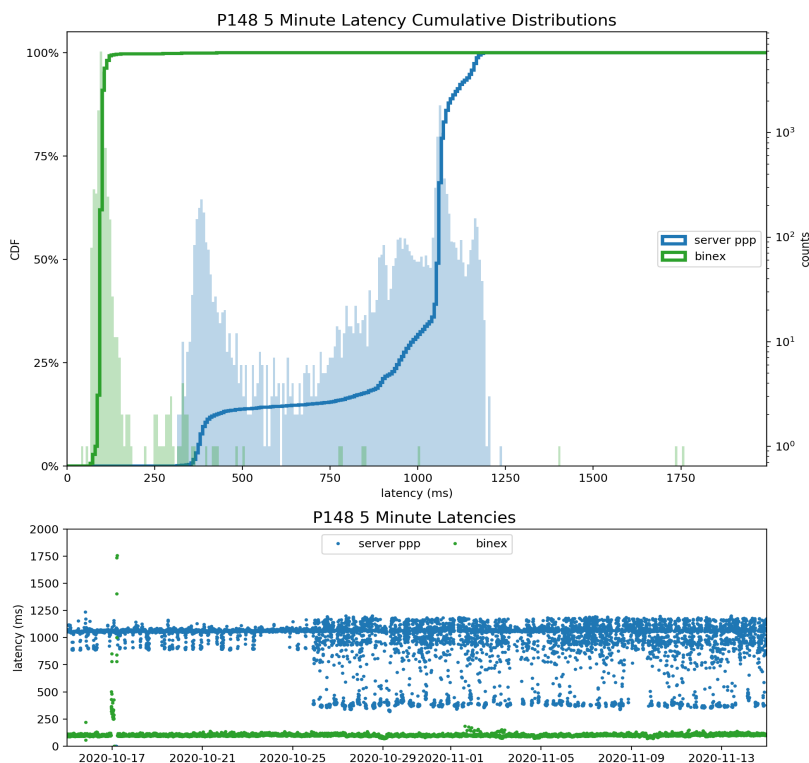


Figure 10. Example of 1 sps, multi-layered (BINEX vs PPP) latency time series and distributions. The green is the “raw” incoming BINEX, and the blue is the Trimble RTX server solutions. The difference in latency between the blue and green represents the delay introduced by the processing engine. The bimodal distribution of the server latencies (blue) was identified as a product of the solutions switching between different processing virtual machines with different PPP synchronization delays. This type of analysis, made possible by the updated temporal and nodal latency sampling resolution, shed light on such an artifact which has since been addressed.

In addition, UNAVCO now stores latency time information at each point in the real-time processing chain at each individual epoch, once per second. Storing this higher resolution, multi-nodal latency information allows network operators to capture real-time streaming performance more accurately. Examples of this improvement include capturing periodic or sporadic stream outages or delays that might be averaged out in the hourly samples and identifying stream processing latency effects such as tuning PPP solution synchronization window delays on the UNAVCO real-time servers to further decrease end-to-end latency (Figure 10). Cumulative

distribution plots derived from higher frequency latency measurements, such as the top panel in Figure 10, enable end users to assess completeness as a function of latency with increased temporal granularity.

b) PPP Solutions

UNAVCO's main real-time processing system, or server-based solutions, uses the Trimble Real Time Extended (RTX) processing engine, which employs the Precise Point Positioning (PPP) methodology. Precise orbit and clock corrections and satellite phase biases are supplied via a continuous stream supplied by Trimble's proprietary CENTERPOINT RTX system. RTX implements real-time precise point position ambiguity resolution (PPP-AR). To accomplish this, the satellite position, clock errors and phase biases supplied in the correction streams are considered known and true. Receiver dependent clock delays and biases are minimized by satellite observation differencing. The tropospheric delay is modelled using a mapping function and the zenith delay is estimated as part of the processing strategy. The integer ambiguities are then derived from the ionosphere-free combinations of the code and phase observations.

The quality of these positions is visualized in several ways: 6-hour windows of scatter plots of horizontal components, and 6-hour windows of time-series plots of the three topocentric components and the three-component displacement vector magnitude are updated every 10 seconds for each station. In addition, drift or "wander" plots are updated daily to capture station-dependent noise signatures over a range of periods. The plots show the WRMS of the displacements in the north, east, and up components across a range of time windows. The wander plots are variograms that can be used to determine if an observed change in displacement over some period differs from the normal variations (Langbein, 2020). The drift plots are the Root-Mean-Square (RMS) of the relative displacement between data points separated by the interval, t , over the previous 48 hours of data.

c) Onboard PPP vs Server PPP Comparisons

To continuously monitor the performance of the ShakeAlert receivers operating onboard positioning algorithms, UNAVCO generates a series of plots daily in which the onboard solutions are compared to the same receiver's Trimble RTX server-based solution (Figure 11). 24-hour time series plots can help identify time-dependent performance degradation or outages, while horizontal scatter plots offer an intuitive visualization of relative spatial performance. Finally, power spectral density (PSD) plots illustrate noise characteristics of the respective processing methods in the frequency domain. These PSDs are generated from the 24 hours of 1 sps data, using a Welch periodogram of 1-hour windows with 50% overlaps. This frequency domain approach offers quantifiable insight into the station- and processing-method-dependent ambient noise floors (Melgar et al., 2020). These noise levels are of particular interest around the range of periods of EEW signals, in addition to identifying the differences between the processing methods of Section 4.

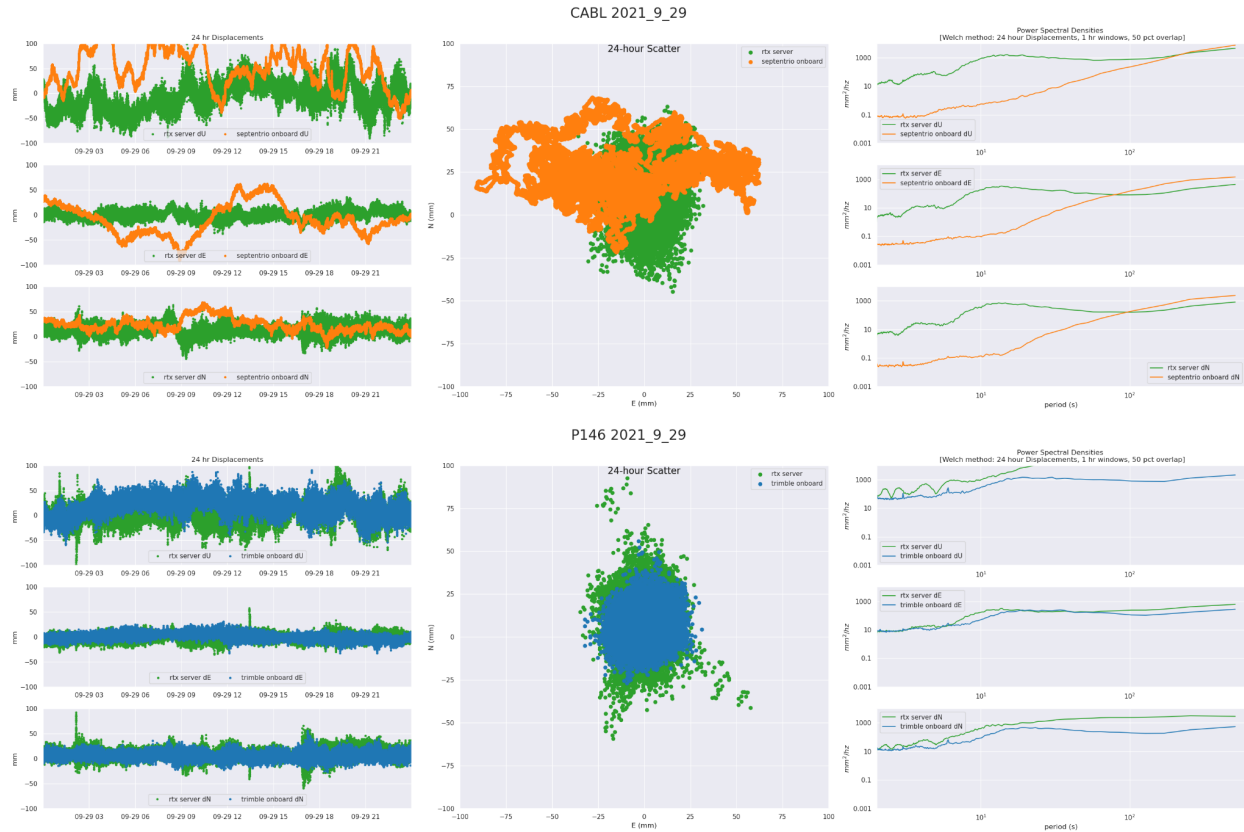


Figure 11: Example summary plots of real-time onboard vs server-based PPP comparisons. The top plots are from CABL, a Septentrio PolaRx5, where orange is the onboard solution and the green corresponds to server-based solution. The bottom plots are from P146, a Trimble NetR9, where blue is the onboard Trimble solution and green corresponds to server-based solution. For links to access these and other plots online see Table 3.

Data availability

As what was previously reported in 2019 (Mattioli et al., 2019), the UNAVCO real-time PPP solutions are broadcast on the rtgpsout.unavco.org on port 2110 of UNAVCO's caster distribution system. The solutions are made available as a NMEA string that contains the station latitude, longitude, and elevation in ITRF08/WGS84 at time of epoch, the UTC date and time, the uncertainty in the north, east and vertical coordinates, number of satellites in the solutions and dilution of precision. The solutions are ingested by USGS (Menlo Park), parsed, and converted to geoJSON for input to the RabbitMQ system. As part of the conversion to geoJSON USGS translates the NOTA RT-GNSS PPP solutions to displacements by comparing the coordinates in the NMEA string to the USGS ShakeAlert master coordinate file.

UNAVCO supplies metadata to enable the separation of the multiplexed NMEA string into separate east, north and height components and the renaming of each component using SEED channel terminology. The UNAVCO real-time database is scanned every 24 hours, and if stations have been added or removed in the ShakeAlert area an updated metadata file is scp'ed to the metadata repository at UC Berkeley (<ftp://www.ncedc.org/outgoing/gps/ShakeAlert/metadata>).

The process is entirely automated. At this time all NOTA real-time stations in Washington, Oregon and California are input to the ShakeAlert metadata file.

The network code for the NOTA real-time stations is “PB.” The displacement channel codes are LYN, LYE, and LYZ. The first character “L” designates it as 1-sps data. The second term “Y” designates it as a processed data set and the third terms N, E and Z represent the north, east and vertical components. The uncertainties are represented by LY1, LY2 and LY3 where the third characters 1, 2 and 3 refer to the uncertainties in the north, east and up components.

Prototype of cloud-based distributed event streaming platform

UNAVCO has begun an ongoing transition to cloud-based data services. A component of this transition includes redesigning the current real-time sensor dataflow into a publisher-subscribe event streaming platform. A prototype of this platform has been implemented in an on-premises compute cluster at UNAVCO and will be migrated to a cloud- or cloud-like-service for primary real-time operations. In this prototype architecture, sensors stream raw data in real-time or near-real-time to containerized Apache Kafka message buses. Internally, a combination of stream processing and Kafka consumers/producers will enable end-users to subscribe to these streams at any point in the processing chain in a variety of formats and translations. In addition, messages will stream into a circularly buffered time-series database to enable low latency, near-real time data retrieval and support real-time monitoring dashboards such as Grafana (Figure 12). This many-to-many streaming architecture will leverage internet of things (IOT) technologies to offer enhanced throughput, fault tolerance and scalability of the UNAVCO real-time contribution to Earthquake Early Warning.

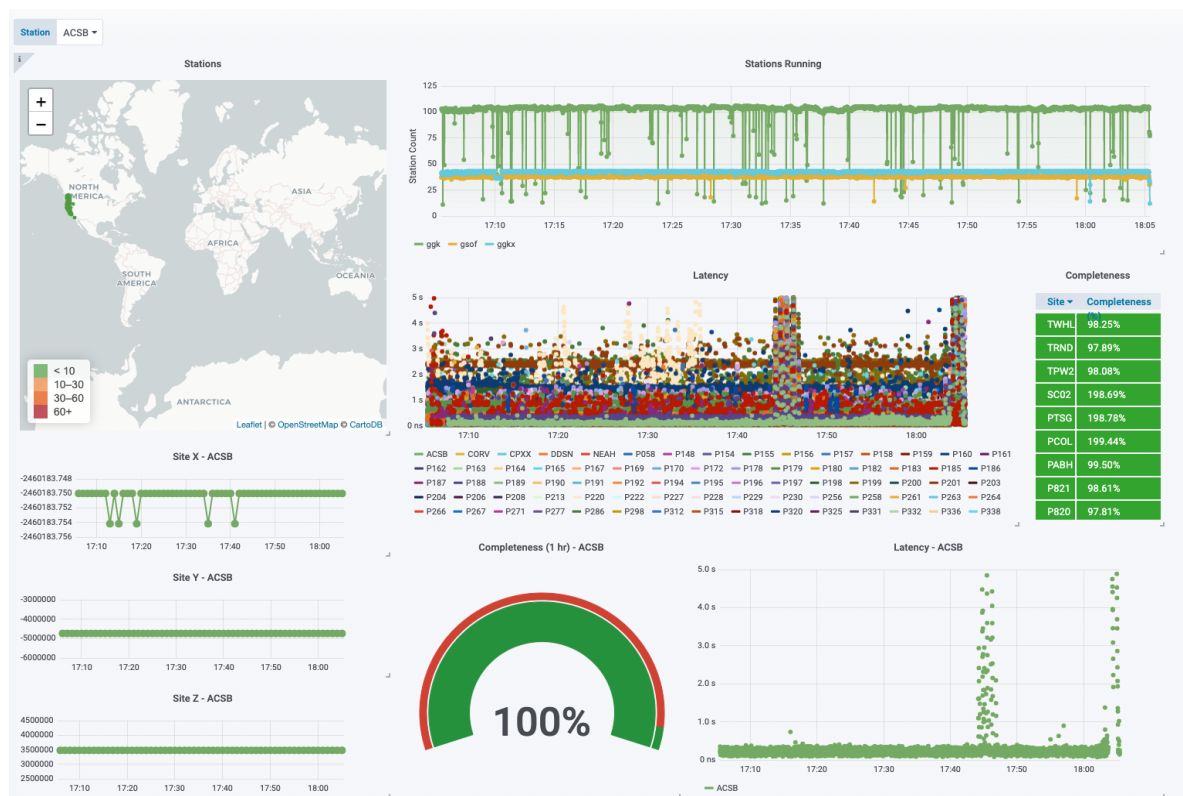


Figure 12: Prototype Grafana dashboard for real-time monitoring of onboard PPP streams

Publications and presentations (2019-2021) arising from this Cooperative Agreement

Austin, K., Mann, D., Woolace, A., Walls, C., Faux, K., Mattioli, G., Dittman, T., Downing, J., Hodgkinson, K., Gallahert, W., Incorporating the Network of the Americas (NOTA) GNSS network into ShakeAlert. American Geophysical Union Fall Meeting 2019, December 2019

Austin, K., Mann, D., Mattioli, G., Feaux, K., Rhoades, S., Mencin, D., Dittmann, T., Sievers, C., Gallaher, W., Incorporating Real-time GNSS into ShakeAlert: Improving Telemetry and Upgrading to Multi-Constellation GNSS with Onboard Positioning at Existing NOTA Stations. AGU American Geophysical Union Fall Meeting 2021, December 2021

Dittmann, S.T., Hodgkinson, K., Mencin, D., Sievers, C. Higher Rate Real-Time GNSS Performance Metrics in the Network of the Americas. SSA Annual Meeting 2020.

Dittmann, S.T., Hodgkinson, K.H., Mencin, D., Sievers, C. Real-time GNSS Quality in the Network of the Americas. AGU Fall Meeting Abstracts 2020, IN038-03

Dittmann, T., Hodgkinson, K., Mencin, D., Sievers, C. Real-Time, Higher Rate NOTA GNSS Analytics and Quality Control. SSA Annual Meeting 2021.

Dittmann, T., Hodgkinson, K., Mann, D., Sievers, C., Mattioli, G., Mencin, D. Quantitative Comparison of Unavco's real-time, 1 Hz GNSS Position Estimates for Earthquake Early Warning. AGU American Geophysical Union Fall Meeting 2021, December 2021

Dittmann, T., Hodgkinson, K., Morton, J., Mencin, D., Mattioli, G. (2021). Comparing Geodetic Processing Methods Sensitivities for Rapid Earthquake Magnitude Estimation. Seismol. Res. Lett. (Submitted for Publication)

Hodgkinson K., Mann, D. NOTA GNSS Positioning for ShakeAlert Network Infrastructure, On-Site and Data Center Solutions. USGS ShakeAlert Research and Development Workshop, Virtual, 25-26 January 2021

Hodgkinson, K., Terry, R., Sievers, C., Dittmann, S., Gottlieb, M. H., et al. The Network of the Americas as a Distributed Event Streaming Platform. SSA Annual Meeting 2021.

Hodgkinson, K., Mencin, D., Walls, C., Mann, D., et al. The 2019 Ridgecrest Earthquake Sequence Tests Integration of Real-Time GNSS for Earthquake Early Warning. SSA Annual Meeting 2020.

Hodgkinson, K. M., D. J. Mencin, K. Feaux, C. Sievers, and G. S. Mattioli (2020). Evaluation of Earthquake Magnitude Estimation and Event Detection Thresholds for Real-Time GNSS Networks: Examples from Recent Events Captured by the Network of the Americas, Seismol. Res. Lett. 91, 1628–1645.

Mattioli, G. S., D. A. Phillips, K. M. Hodgkinson, C. Walls, D. J. Mencin, B. A. Bartel, D. J. Charlevoix, C. Crosby, M. J. Gottlieb, B. Henderson, et al. (2020). The GAGE Data and Field

Response to the 2019 Ridgecrest Earthquake Sequence, *Seismol. Res. Lett.* XX,1–12, doi: 10.1785/0220190283.

Pyatt, C., Arnoux, G., Austin, K., Downing, J., Faux, K., Mann, D., Mattioli, G., Rhoades, S., Woolace, A. ShakeAlert GNSS Data Coverage Densification on the Oregon Coast. Gage/Sage 2021 Community Science Workshop, Virtual, 9-13 August 2021

Pyatt, C., Arnoux, G., Austin, K., Downing, J., Faux, K., Mann, D., Mattioli, G., Rhoades, S., Woolace, A. ShakeAlert: Closing the NOTA GNSS Coverage Gap along the Oregon Coast. AGU American Geophysical Union Fall Meeting 2021, December 2021

Terry, R., Sievers, C., Gottlieb, M., Dittmann, T., Hodgkinson, K., Mencin, D. Redesigning and modernizing UNAVCO's real-time GNSS streaming architecture. GAGE/SAGE 2021 Community Science Workshop.

References Cited

Langbein, J. (2020). Methods for rapidly estimating velocity precision from GNSS time series in the presence of temporal correlation: a new method and comparison of existing methods. *Journal of Geophysical Research: Solid Earth*, 125, e2019JB019132. <https://doi.org/10.1029/2019JB019132>

Mattioli, G., Feaux, K., Mann, D., Hodgkinson, K., Downing, J. (2019). Incorporating Real-Time GNSS into ShakeAlert: Improving Telemetry, Reducing Latency, and Enhancing Robust GNSS Data Flow at Existing PBO Stations in CA, OR, and WA. Final Technical Report, USGS Cooperative Agreement (G17AC00313) https://earthquake.usgs.gov/cfusion/external_grants/reports/G17AC00313.pdf

Melgar, D., Crowell, B. W., Melbourne, T. I., Szeliga, W., Santillan, M., & Scrivner, C. (2020). Noise characteristics of operational real-time high-rate GNSS positions in a large aperture network. *Journal of Geophysical Research: Solid Earth*, 125, e2019JB019197.

Acknowledgement of Support

This material is based upon work supported by the U.S. Geological Survey under Cooperative Agreement No. G19AC00287. UNAVCO operates the Enabling Discoveries in Multiscale Earth System Dynamics: Geodetic Facility for the Advancement of Geoscience (GAGE) (Master CA-1724794). Core support for the operation of the Network of the Americas (NOTA) is from the NSF as part of the GAGE Facility.

Disclaimer

The views and conclusions contained in this document are those of the authors and should not be interpreted as representing the opinions or policies of the U.S. Geological Survey. Mention of trade names or commercial products does not constitute their endorsement by the U.S. Geological Survey